Journal of Catalysis 273 (2010) 229–235

Contents lists available at ScienceDirect

Journal of Catalysis

journal homepage: www.elsevier.com/locate/jcat

Water-induced formation of cobalt oxides over supported cobalt/ceria–zirconia catalysts under ethanol-steam conditions

Sean S.-Y. Lin [a,1], Do Heui Kim [b], Mark H. Engelhard [c], Su Y. Ha [a,*]

[a] The Gene and Linda Voiland School of Chemical Engineering and Bioengineering, Washington State University, P.O. Box 642710, Pullman, WA 99164-2710, USA
[b] Institute for Interfacial Catalysis, Pacific Northwest National Laboratory, P.O. Box 999, Richland, WA 99354, USA
[c] Environmental Molecular Sciences Laboratory, Pacific Northwest National Laboratory, P.O. Box 999, Richland, WA 99354, USA

ARTICLE INFO

Article history:
Received 14 January 2010
Revised 22 April 2010
Accepted 25 May 2010
Available online 30 June 2010

Keywords:
Ethanol steam reforming
Hydrogen production
Cobalt oxides
Ceria–zirconia
In situ TPR
In situ XPS
CO chemisorption

ABSTRACT

The water-induced formation of cobalt oxides by the re-oxidation of metallic cobalt in pre-reduced 10% Co/CeO_2–ZrO_2 catalyst was verified by in situ temperature-programmed reduction (TPR) and in situ X-ray Photoelectron Spectroscopy (XPS) studies under various ethanol-steam conditions at 450 °C. The formation and transformation of water-induced cobalt oxide species during the reaction were influenced by the pre-reduction conditions as well as the feed stream composition. Our results suggest that the surface composition of the cobalt species (e.g. Co, CoO, and CoO_x) in the 10% Co/CeO_2–ZrO_2 catalyst, initially determined by the catalyst pre-treatment conditions, changed toward an equilibrium state governed by the feed stream composition as the reaction proceeded. In addition, the reducibility of the ceria sites may play a significant role in the formation of such water-induced cobalt oxide species, as the redox process involves both cobalt and ceria sites in the ethanol-steam environment. Finally, the effect of the water-induced cobalt oxides in the 10% Co/CeO_2–ZrO_2 catalyst was investigated under ethanol and ethanol-steam conditions, particularly for the carbon–carbon (C–C) bond cleavage of ethanol. The water-induced formation of cobalt oxides in the catalyst was not observed to affect the cleavage, in either ethanol-rich (e.g. ethanol decomposition) or steam-rich (e.g. ethanol steam reforming) conditions. This result could be explained by our in situ studies, which revealed the redox exchange between reduced cobalt and oxidized cobalt in a feed stream with a changing water-to-ethanol ratio.

Published by Elsevier Inc.

1. Introduction

Catalysts for hydrogen production through ethanol steam reforming (ESR) have been carefully studied and summarized in the recent literature [1–4]. Precious metals such as Rh, Pt, and Pd have been found to be effective catalysts. Rh, in particular, is the most active because the formation of five-member ring oxametallacycles over Rh surfaces during the dehydrogenation of ethanol facilitates the C–C bond cleavage of the adsorbed ethoxide species, when compared with the acetaldehyde formed over Pd surfaces, which can lead to acetone formation [5,6]. However, larger-scale applications of ESR would be impractical using expensive Rh-based catalysts.

As an inexpensive alternative for ethanol reforming applications, Co-based catalysts have attracted much attention recently; their activity for efficient C–C bond cleavage around 400 °C has been reported to be similar to that of precious metal catalysts [7,8]. The similarity in terms of activity for the C–C bond cleavage is not surprising, as revealed by density function theory (DFT) calculations that the oxametallacyclic intermediate is more stable over Rh and Co surfaces than over other transition metals [6].

In addition, the catalytic properties of Co-based catalysts that determine the reaction turnovers and the product selectivity in a kinetic-controlled regime during ESR are found to be strongly influenced by the supporting materials, such as Al_2O_3, MgO, ZnO, SiO_2, and ZrO_2 [7–11]. The Co-support interactions and their influence on catalytic performance over supported Co catalysts have been a research focus in the steam reforming of ethanol. Based on what has been found in supported metal catalysts [12] and our previous findings [13,14], it is generally believed that C–C bond cleavage takes place on metallic Co surfaces, while the support plays a dual role, physically stabilizing Co nanocrystallites and chemically facilitating the oxidation process by activating water molecules or releasing lattice oxygen.

Although metallic Co was shown to be responsible for the activity in several ethanol reforming studies using bulk and supported Co catalysts [14–18], owing to the difficulty of characterizing Co species over support surfaces in *operando* conditions, the true identity of its active centers in ESR is still elusive. Furthermore, the

---

[*] Corresponding author.
E-mail address: suha@wsu.edu (S.Y. Ha).
[1] Present address: Department of Chemical and Biological Engineering, Northwestern University, 2145 Sheridan Rd., Tech E-136, Evanston, IL 60208-3120, USA.

0021-9517/$ - see front matter Published by Elsevier Inc.
doi:10.1016/j.jcat.2010.05.016

coexistence of metallic Co and Co oxides (CoO_x) was observed and seems unavoidable in a steam-rich environment given by a high steam-to-carbon feed condition; it is a challenging task to differentiate cobalt species with different oxidation states and correlate the composition of the bulk cobalt to catalytic properties, especially when they are coupled with Co-support interactions.

The presence of CoO_x, or more precisely, the re-oxidation of metallic Co to CoO_x, is also an interesting topic in supported Co-based Fischer–Tropsch catalysts. The negative effect of water on catalyst activity in Fischer–Tropsch synthesis could be linked to the formation of inactive cobalt oxides; however, the issue remains controversial [19–23]. In the case of ESR, however, very few papers address the effect of water on the oxidation of cobalt, and the discussion is mostly limited to the bulk cobalt catalysts [16,17]. The assumption that the metallic cobalt is stable and acts as the active center is generally made in studies of supported cobalt catalysts for ESR, in which the activity and stability are measured, and the cobalt-support interactions are discussed for the pre-reduced metallic cobalt only. Therefore, in steam reforming conditions or reactions involving steam, the redox exchange between the reduced and oxidized cobalt species and their interactions with support surfaces as well as adsorbed molecules should not be overlooked, as the nature of the active sites is still under investigation.

This work examines the formation of CoO_x species over supported $Co/CeO_2–ZrO_2$ catalysts in different ethanol-steam conditions including ethanol steam reforming, water-assisted ethanol decomposition, and ethanol decomposition reactions. Supported $Co/CeO_2–ZrO_2$ was chosen as a model catalyst system because its high activity toward hydrogen production via ethanol steam reforming has been shown to be closely related to the reducibility of cobalt and the cobalt-support interactions [13,24].

Several in situ techniques including diffuse-reflectance infrared Fourier transform spectroscopy (DRIFTS), temperature-programmed reduction (TPR), and X-ray Photoelectron Spectroscopy (XPS) were used to characterize the formation of water-induced CoO_x over supported $Co/CeO_2–ZrO_2$ in various ethanol-steam mixtures. The re-oxidation of metallic Co and a transient exchange between metallic Co and CoO_x were found to be associated with water-to-ethanol ratios in the feed stream. Furthermore, the Co–Ce interaction in the catalyst was demonstrated, as the extent of reduction for the Ce species in the $CeO_2–ZrO_2$ support was found to play a key role in the re-oxidation/re-reduction of the supported cobalt species in ethanol-steam conditions.

2. Experimental

2.1. Catalyst preparation and activity evaluation

Incipient wetness impregnation was used for the synthesis of supported $Co_3O_4/CeO_2–ZrO_2$. Commercial nanocrystalline $CeO_2–ZrO_2$ (Ce/Zr atomic ratio close to 3, Sigma-Aldrich) was impregnated with cobalt nitrate, $Co(NO_3)_2·6H_2O$ (Alfa Aesar), followed by calcination at 500 °C in air for 4 h to form supported cobalt oxides on $CeO_2–ZrO_2$ (10 wt.% cobalt). This sample is denoted as 10% Co–CZ. A detailed characterization of the physical properties of this catalyst, such as crystalline structure, surface area, pore volume, and morphology, has been carried out in our previous study [24].

The catalytic activity of 10% Co–CZ was evaluated in a series of catalyst testing experiments. Approximately 100 mg catalyst was charged into an 8-mm-ID quartz packed-bed reactor inside a Watlow temperature-controlled furnace at atmospheric pressure. Gas flows were controlled with Brooks Mass Flow Controllers (Model 5850E). The catalyst was pre-reduced under 20 sccm hydrogen flow at 450 °C for 2 h before the activity evaluation. After the pre-reduction, degassed ethanol or a degassed ethanol–water mixture was injected into the reactor with a syringe pump and vaporized in a pre-heater containing an SiC bed with a 10-sccm helium carrier gas. Ethanol was fed at a constant weight hourly space velocity (WHSV) of 1.58 h^{-1} in all the streams. The product stream was passed through a two-stage condenser to remove water, unconverted ethanol, and any other possible liquid by-products before the gas analysis. The effluent composition was analyzed using an SRI gas chromatograph equipped with a thermal conductivity detector (TCD), molecular sieve 13X, and Hayesep D columns, capable of separating and measuring H_2, CH_4, CO, CO_2, C_2H_6, and C_2H_4. The catalyst performance was analyzed in terms of the carbon–carbon (C–C) cleavage conversion of ethanol and the formation rate of gaseous products. This rate was calculated on the basis of the catalyst mass. The C–C cleavage conversion of ethanol was defined using a carbon basis molar ratio, the ratio of gaseous C1 compounds (CH_4, CO, and CO_2) in the product stream to the ethanol in the feed stream:

$$\text{C—C cleavage conversion}(\%) = \left(\frac{CH_4 + CO + CO_2}{C_2H_5OH \times 2}\right) \times 100$$

2.2. In situ TPR

Temperature-programmed reduction (TPR) experiments were performed using a Micromeritics ChemiSorb 2720 equipped with a thermal conductivity detector (TCD). In a typical in situ TPR experiment, approximately 40 mg of sample was held by quartz wool and placed in a U-shaped quartz tube, where a syringe pump delivered an ethanol–water mixture through a customized stainless tube (0.042″ OD and 0.027″ ID) positioned above the sample . Thermocouples were directly in contact with the quartz tube of the sample section. The H_2-TPR profiles were recorded at a ramping rate of 10 °C/min from 25 °C to 850 °C and a 40-sccm flow rate of 10% H_2–Ar mixture. Depending on the measurement type, different thermal pre-treatments were used before the H_2-TPR profile was recorded. The sample was pre-oxidized for all the measurements to eliminate possible surface contamination before the pre-reduction and titration procedures. The sample was pre-oxidized at a 40-sccm flow rate of 5% O_2-helium at 500 °C for 30 min. Pre-reduction of the sample was performed at a 40-sccm flow rate of the 10% H_2–Ar mixture at a desired temperature for 1 h. The water titration or ethanol–water titration was performed at a 40-sccm flow rate of Ar at 450 °C with a liquid volume of 0.025 ml at a feed rate of 0.5 ml/h. The liquid (water or ethanol–water) for the titration was degassed to remove any dissolved O_2. The blank H_2-TPR profile was obtained by carrying out the same procedure (pre-oxidation, pre-reduction, water titration) over a sample tube filled only with quartz wool to ensure there was no interference in the TCD signal.

2.3. In situ DRIFTS

CO chemisorption was carried out by diffuse-reflectance infrared Fourier transform spectroscopy (DRIFTS) using a Perkin-Elmer System 2000 FTIR spectrometer with a liquid-nitrogen-cooled MCT detector. A Harrick Scientific HVC-DR2 reaction chamber mounted inside the spectrometer provided temperature-controlled flow-through atmospheres for catalyst pre-treatments for CO chemisorption. The path of the infrared beam inside the sample compartment was purged with nitrogen to eliminate water and CO_2 noise during the measurements.

Three different pre-treatments were used for the sample powders (~140 mg) before CO chemisorption. A hydrogen or helium flow of 30 sccm was introduced into the reactor chamber at

400 °C for 2 h to reduce or dehydroxylate the sample surfaces. The removal of the surface-bound water was confirmed by monitoring the mass loss using thermogravimetric analysis (TGA) under the same thermal pre-treatment. In the case of water pre-treatment, a 2% water-helium stream generated by a gas-bubbling system was introduced over the sample for 1 h following the H_2 pre-reduction at 400 °C for 2 h. In order to eliminate any possible surface-bound species generated during the pre-treatment, sample powders were purged with helium at 400 °C for 2 h then cooled to 35 °C to obtain a background spectrum. Finally, a certified 2% CO-helium stream of 30 sccm was introduced over the sample powders at 35 °C. The DRIFTS spectra of gaseous species and adsorbed species were measured every five minutes for 1.5 h. They were collected by adding 128 scans in four minutes with a resolution of 4 cm^{-1} in each measurement.

2.4. In situ XPS

In situ XPS measurements were carried out in a catalytic side chamber designed in house attached to a Physical Electronics Quantum 2000 Scanning ESCA Microprobe. Sample powders were thermally treated in the catalytic side chamber and transferred in vacuo to an analyzer for measuring photoelectron energy spectra. This system uses a focused monochromatic Al Kα X-ray (1486.7-eV) source and a spherical section analyzer. The instrument has a 16-element multichannel detector. The X-ray beam used was a 100-W, 100-μm-diameter beam, which was rastered over a 1.3 mm by 0.2 mm rectangle on the sample. The X-ray beam is incident normal to the sample, and the photoelectron detector was at 45° off normal, using an analyzer angular acceptance width of 20°×20°. Wide scan data were collected using a pass energy of 117.4 eV. The binding energy (BE) scale was calibrated using the Cu2$p_{3/2}$ feature at 932.62 ± 0.05 eV and Au 4f at 83.96 ± 0.05 eV for known standards. The sample experienced variable degrees of charging. Low-energy electrons, at ~1 eV, 20 μA, and low-energy Ar^+ ions were used to minimize this charging. The BE scale was referenced to the Ce3$d_{3/2}$ 4f^0 line for Ce^{4+} at 917.0 eV.

3. Results and discussion

3.1. Water-induced oxidation of pre-reduced cobalt species

The typical H_2-TPR experiments were carried out for the 10% Co–CZ catalyst with and without the pre-reduction, and three different reduction temperatures (350, 450, 550 °C) were used to study the bulk reduction behavior. As can be seen in Fig. 1a, the TPR profile of the sample without the pre-reduction (as calcined) shows two reduction peaks (275 and 366 °C), which can be attributed to the reduction of cobalt oxides, $Co^{3+} \rightarrow Co^{2+}$ and $Co^{2+} \rightarrow Co^0$, respectively [24]. In addition, a third peak (472 °C), hidden in the shoulder of the second peak, is associated with the surface reduction of the ceria species in the CeO_2–ZeO_2 support [24]. As shown in the H_2-TPR profiles, after a H_2 pre-reduction of 2 h, most of the supported cobalt species were reduced to metallic cobalt; the residual cobalt oxides are indicated by the small reduction peak between 250 and 300 °C. Moreover, the peak that is attributed to the CeO_2–ZeO_2 support (472 °C) disappeared for the samples pre-reduced at 450 °C or higher, indicating the reduction of the surface ceria species in CeO_2–ZeO_2 at such temperatures.

To study the ability of water to oxidize CeO_2–ZrO_2-supported Co species, in situ H_2-TPR experiments were carried out over the 10% Co–CZ samples that had been individually pre-reduced at different temperatures (350, 450, 550 °C) and then treated with water at 450 °C; the CeO_2–ZrO_2 support was used to provide a basis for the effect of water titration on the pre-reduced Co species of the catalyst. According to Fig. 1b, the 10% Co–CZ samples that had been H_2 pre-reduced as well as water-titrated show the H_2-TPR reduction peaks below 400 °C, while the in situ H_2-TPR profile of CeO_2–ZrO_2 support shows no reduction peaks below 400 °C. Thus, the reduction peaks below 400 °C depict the formation of water-induced cobalt oxides in the pre-reduced 10% Co–CZ sample, which can be further categorized as type I CoO_x (50–150 °C) and type II CoO_x (150–350 °C) according to their reducibility as shown in the H_2-TPR profiles. The nature of these cobalt oxides, however, needs further characterization.

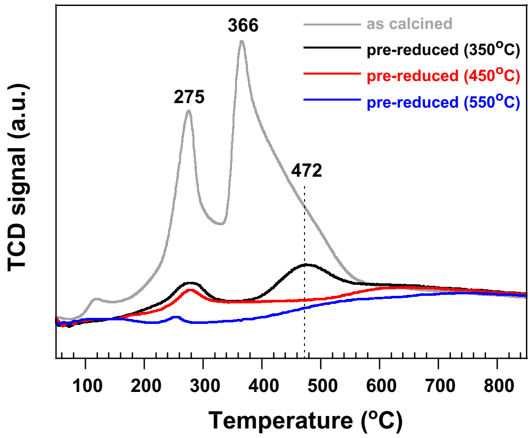

Fig. 1a. H_2-TPR profiles of the 10% Co/CeO_2–ZrO_2 (40 mg) as calcined in air at 500 °C for 4 h, and the 10% Co/CeO_2–ZrO_2 (40 mg) as pre-reduced in 10% H_2/Ar (40 sccm) at 350 °C, 450 °C, and 550 °C for 1 h, respectively. Before the H_2-TPR measurements, all the samples were pre-treated in 5% O_2-helium (40 sccm) at 500 °C for 30 min.

Based on the experimental observations from our in situ H_2-TPR study, the formation of type I CoO_x was suggested to be linked to the Co–Ce interaction in the catalyst. First, in a separate in situ H_2-TPR experiment for supported 10% Co/ZrO_2 catalyst carried out under the same conditions as those used for generating Fig. 1b, the formation of type I CoO_x was not seen on the ZrO_2-supported sample. A comparison, shown in Fig. 1c, indicates that the ceria species might be partly responsible for the formation of type I CoO_x in the 10% Co–CZ catalyst. Second, the formation of type I and type II CoO_x was shown to be influenced by the degree of reduction for CeO_2–ZrO_2 species. This can be seen in Fig. 1b: when

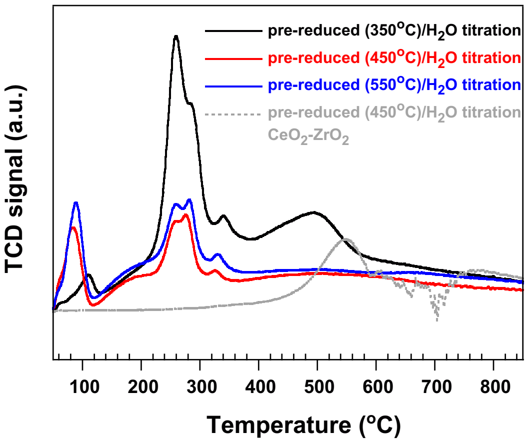

Fig. 1b. In situ H_2-TPR profiles of the 10% Co/CeO_2–ZrO_2 (40 mg) and the CeO_2–ZrO_2 (40 mg) as pre-reduced in 10% H_2/Ar (40 sccm) at 350, 450, and 550 °C followed by an in situ H_2O titration in Ar (40 sccm) at 450 °C with a liquid volume of 0.025 ml at a feed rate of 0.5 ml/h.

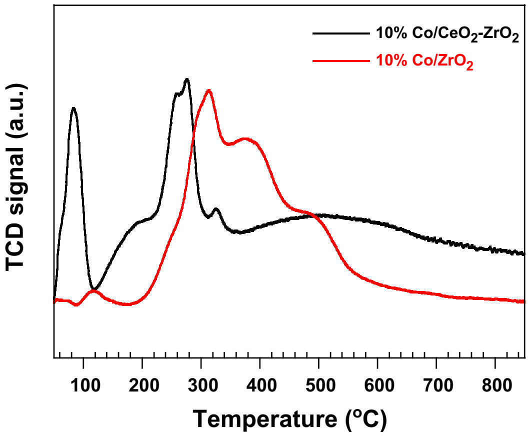

Fig. 1c. In situ H_2-TPR profiles of the 10% Co/CeO_2–ZrO_2 (40 mg) and the 10% Co/ZrO_2 (40 mg) as pre-reduced in 10% H_2/Ar (40 sccm) at 450 °C followed by an in situ H_2O titration in Ar (40 sccm) at 450 °C with a liquid volume of 0.025 ml at a feed rate of 0.5 ml/h.

a lower pre-reduction temperature (350 °C) was used, less type I CoO_x formed, and a higher concentration of type II CoO_x coexisted with unreduced CeO_2–ZrO_2 species. As higher pre-reduction temperatures (e.g. 450 °C and higher) were used, more type I CoO_x formed at the expense of the formation of type II CoO_x, and the reduction peak of CeO_2–ZrO_2 species disappeared, indicating that most surface Ce species were reduced. Therefore, it is apparent that when the pre-reduced catalyst was further treated with water, the reduced Ce species of the CeO_2–ZrO_2 support could interact with metallic Co species, and this interaction could be the key step that leads to the formation of type I CoO_x as seen in Fig. 1b. However, it is not yet clear how the surface Ce species interacted with the adjacent Co species in the presence of water molecules. The formation of type I and type II CoO_x has also been shown to be associated with the concentration of water in the ethanol–water titration process and will be discussed in a later section.

In addition to the in situ H_2-TPR technique, CO chemisorption using in situ DRIFTS was carried out for the 10% Co–CZ catalyst to characterize the formation of water-induced CoO_x from the pre-reduced Co species. The catalyst was pre-treated with the same thermal treatment in different atmospheres (helium, H_2, H_2–H_2O) before it was examined using CO chemisorption. The three spectra shown in Fig. 2a were obtained from the samples pre-treated at 400 °C in (a) H_2, (b) H_2 followed by water titration or (c) helium. CO chemisorption at 35 °C over these pre-treated samples resulted in complicated absorption bands in the range of 1000–1800 cm^{-1}; these bands are attributed to symmetric or asymmetric O–C–O vibrations originating from monodentate, bidentate, polydentate, and bridged carbonates [25–27]. Identifying individual species is not a straightforward task; however, the differences between their peak intensities can be directly linked to the coverage with adsorbed carbonate species of the pre-treated catalyst surfaces (i.e. higher surface carbonate concentration leads to higher peak intensities).

Catalyst pre-treatment that changes the concentration of the surface metal–oxygen bonds leads to coordinatively unsaturated surfaces and affects the amount of carbonate formation during CO chemisorption. The more reduced sample shown in Fig. 2a (spectrum a) has the least carbonate formation because most of the Co oxides were reduced to metallic Co (Co^0), which provides fewer surface sites for CO to form surface carbonates. The sample that was dehydroxylated in helium without further reduction preserved oxygen-rich surfaces to give a large amount of carbonate formation after CO chemisorption, as shown in Fig. 2a (spectrum c).

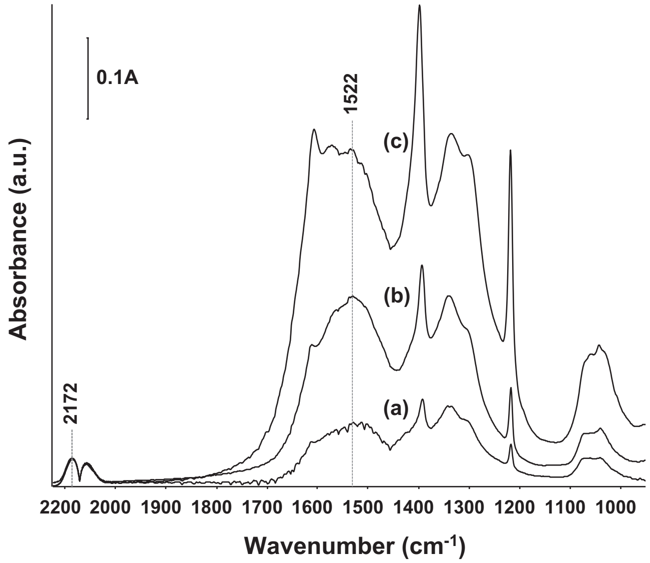

Fig. 2a. DRIFTS spectra of CO chemisorption over 10% Co/CeO_2–ZrO_2 (140 mg) at 35 °C in 2% CO-helium (30 sccm) for 1.5 h: (a) pre-reduced at 400 °C in H_2 (30 sccm) for 2 h; (b) pre-reduced at 400 °C in H_2 for 2 h followed by H_2O titration in 2% H_2O-helium (30 sccm) at 400 °C for 1 h; (c) pre-treated at 400 °C in helium (30 sccm) for 2 h.

The effect of water titration on carbonate formation over the catalyst can be seen by comparing spectrum (a) with spectrum (b) in Fig. 2a. The fact that more carbonate formed on the water-titrated surface than on the pre-reduced surface suggests the re-oxidation of Co species by water. A clearer comparison can be seen in Fig. 2b, where the dynamic changes in the peak heights of the surface-bound carbonates (1522 cm^{-1}) and gaseous CO (2172 cm^{-1}) were recorded during CO chemisorption over the pre-treated catalysts. As shown, the peak intensity of gaseous CO is close to constant in all the samples, indicating that the substrate reflectances of all the samples are comparable for reliable IR measurements; hence, the difference in peak height of carbonates must truly be

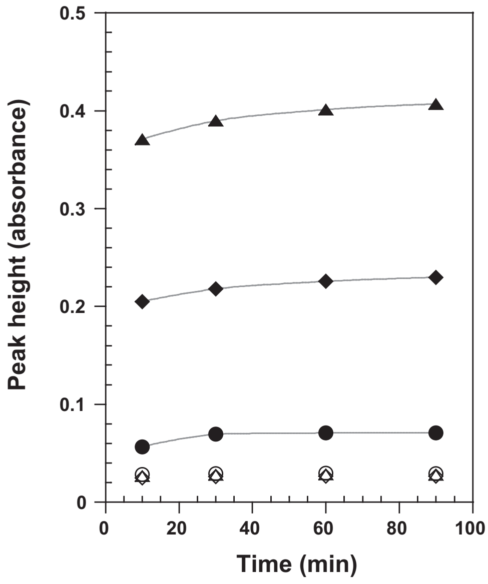

Fig. 2b. DRIFTS peak evolutions of the surface carbonates (1522 cm^{-1}, solid marks) and the gaseous CO (2172 cm^{-1}, open marks) over the 10% Co/CeO_2–ZrO_2 samples at 35 °C during CO chemisorption: pre-reduced in H_2 at 400 °C (●); pre-reduced in H_2, followed by H_2O titration at 400 °C (◆); pre-treated in helium at 400 °C (▲).

caused by the sample pre-treatments that modified the oxidation state of the surface cobalt species. Moreover, a difference in the amount of carbonates is not seen in Fig. 2c, where the same comparison is made for CeO_2–ZrO_2, showing that water titration mainly oxidized cobalt species, since the pre-reduction temperature of 400 °C may not be sufficient for reducing CeO_2–ZrO_2.

3.2. Transient oxidation/reduction of cobalt species in ethanol–water mixtures

As discussed in the previous section, the formation of water-induced Co oxides over the 10% Co–CZ catalyst has been confirmed using in situ TPR and CO chemisorption. It was found that the surface state of the pre-reduced catalyst, particularly the Co–Ce interactions, influenced the re-oxidation of the pre-reduced Co species during water titration.

Using in situ TPR and in situ XPS techniques, it was also found that, in an ethanol–water environment that simulates real reaction conditions (i.e. ethanol decomposition, water-assisted ethanol decomposition, and ethanol steam reforming reactions), the formation of water-induced Co oxides over 10% Co–CZ catalysts is subject to the water-to-ethanol ratio in the feed stream.

Fig. 3 shows the H_2-TPR profiles for the 10% Co–CZ catalysts that were pre-reduced, followed by an in situ titration with ethanol, water, or ethanol–water mixture at 450 °C. As demonstrated in Fig. 1b, the peaks attributed to type I and type II CoO_x, also shown in Fig. 3, indicate the formation of water-induced CoO_x after the catalyst was titrated with an ethanol–water mixture. The water-to-ethanol ratio used in the mixture, indicative of the oxidizing power of the mixture, appreciably influenced the concentration and the reducibility of type I and type II CoO_x, as shown in their H_2-TPR profiles in Fig. 3.

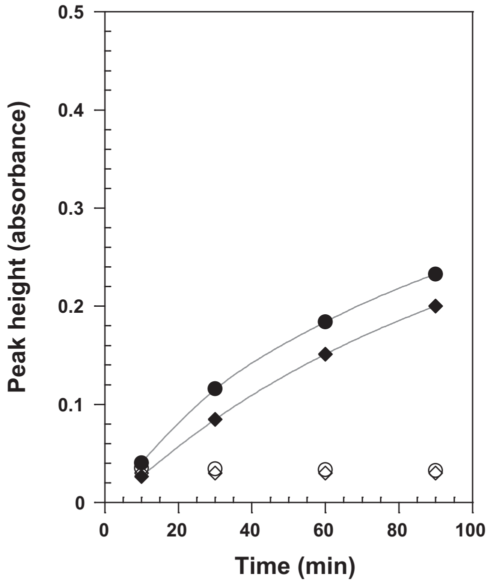

Fig. 2c. DRIFTS peak evolutions of the surface carbonates (1522 cm^{-1}, solid marks) and the gaseous CO (2172 cm^{-1}, open marks) over the CeO_2–ZrO_2 samples at 35 °C during CO chemisorption: pre-reduced in H_2 at 400 °C (●); pre-reduced in H_2, followed by H_2O titration at 400 °C (♦).

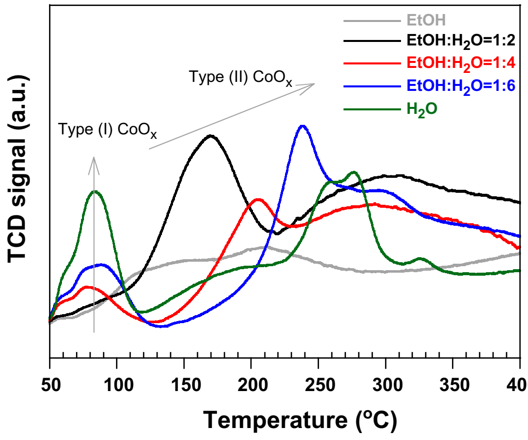

Fig. 3. H_2-TPR profiles of the 10% Co/CeO_2–ZrO_2 (40 mg) as pre-reduced in 10% H_2/Ar (40 sccm) at 450 °C for 1 h followed by an in situ titration in Ar (40 sccm) at 450 °C using ethanol, water, or ethanol–water mixtures with a liquid volume of 0.025 ml at a feed rate of 0.5 ml/h.

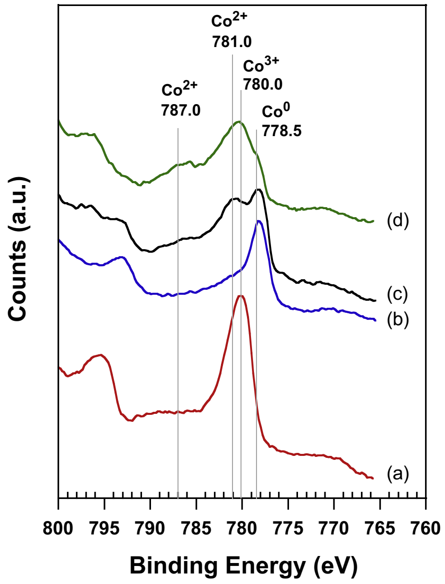

Fig. 4a. In situ XPS spectra (Co2p region) of the 10% Co/CeO_2–ZrO_2 catalyst (a) as calcined in air at 500 °C for 4 h, and as exposed to different feed conditions at 450 °C: (b) H_2 (110 torr) for 4 h, (c) water (20 torr) for 1 h, and (d) water (20 torr)/ethanol (5 torr) for 2.5 h.

The change of oxidation state of Co over the 10% Co–CZ catalyst, indicative of the re-oxidation/re-reduction processes of the pre-reduced Co species, was observed through an in situ XPS study under feed conditions using different water-to-ethanol ratios. Fig. 4a and Fig. 4b show the Co2p and Ce3d XPS spectra obtained from in situ measurements for the 10% Co–CZ catalyst, respectively. Before the respective XPS measurements shown in Fig. 4a and Fig. 4b(a–d) were taken, the catalyst was exposed to the reaction conditions in the following order: (a) vacuum at room temperature; (b) H_2 (110 torr) at 450 °C for 4 h; (c) water (20 torr) at 450 °C for 1 h; (d) water (5 torr)/ethanol (20 torr) at 450 °C for 2.5 h.

Fig. 4a (a) features a peak at 780.0 eV, indicating that the surface Co species of the 10% Co–CZ (i.e. 10% Co/CeO_2–ZrO_2 as calcined in air at 500 °C) was mainly Co^{3+}. After the catalyst was heated in H_2 at 450 °C for 4 h, a peak attributed to Co^0 developed at 778.5 eV, as shown in Fig. 4a (b), indicating the surface of supported cobalt oxide species was mostly reduced to metallic cobalt (Co^0). When water vapor was later introduced over the catalyst at 450 °C for 1 h, the re-oxidation of the Co^0 species gradually occurred and resulted in two additional peaks attributed to Co^{2+}, at 787.0 and 781.0 eV, as shown in Fig. 4a (c). Finally, the sample was exposed to a mixed stream with a water-to-ethanol ratio of 4 at 450 °C for 2.5 h. This condition was chosen to simulate a typical reaction environment for ethanol–water reactions, in which a reducing or H_2-rich environment would be expected because decomposition, dehydrogenation, or steam reforming of ethanol would be likely

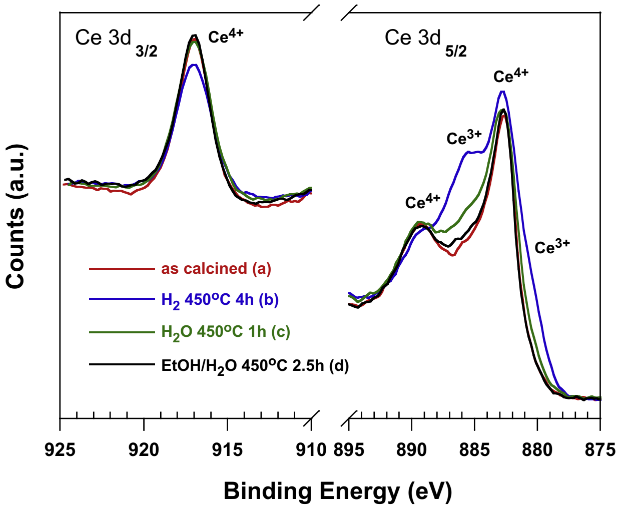

Fig. 4b. In situ XPS spectra (Ce3d region) of the 10% Co/CeO_2–ZrO_2 (40 mg) (a) as calcined in air at 500 °C, and as exposed to different feed conditions at 450 °C: (b) H_2 (110 torr) for 4 h, (c) water (20 torr) for 1 h, and (d) water (20 torr)/ethanol (5 torr) for 2.5 h.

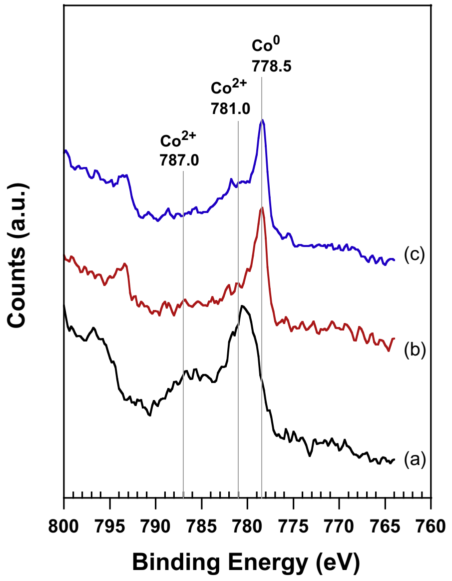

Fig. 4c. In situ XPS spectra (Co2p region) of the 10% Co/CeO_2–ZrO_2 catalyst were obtained in sequence: (a) pre-reduced in 5% H_2-helium at 350 °C (2 torr) for 1 h, (b) exposed to ethanol (10 torr) for 10 min at 450 °C, and (c) exposed to water (12 torr)/ ethanol (1 torr) at 450 °C for 1 h.

to generate H_2 over catalyst surfaces at 450 °C. The catalyst tested using the same conditions (i.e. water-to-ethanol ratio and reaction temperature) typically yielded H_2 around 60–65% of the dry product stream in our study. As Fig. 4a (d) shows, however, more Co^0 was oxidized to Co^{2+}, indicating that the presence of ethanol (i.e. 5 torr ethanol mixed with 20 torr water) has little effect on the occurrence of the re-oxidation process of Co species by water.

It is not yet clear whether ethanol molecules preferentially adsorb on Co sites in a supported Co catalyst system during ethanol steam reforming. Nevertheless, the re-oxidation of Co species in the ethanol–water mixture shown in our in situ XPS results suggests a strong possibility of incoming water molecules forming strong bonds with metallic cobalt sites, resulting in further oxidation.

For Ce species, the change in oxidation state followed a trend similar to that of Co species under in situ conditions. In Fig. 4b, the reduction of Ce in H_2 at 450 °C (i.e. Ce in the CeO_2–ZrO_2 support of 10% Co–CZ) generated Ce^{3+} species from Ce^{4+} species on the catalyst surfaces, which can be seen in the changes in the peak features at 885.8 eV (Ce^{3+}) and 917.2 eV (Ce^{4+}). By monitoring these features in Ce3d spectra, the re-oxidation of the Ce^{3+} species was observed as water was introduced over the catalyst surface at 450 °C. The re-oxidation of Ce^{3+} continued to occur in a mixture of water and ethanol, a result similar to that seen for Co species in their Co2p spectra (Fig. 4a).

These in situ XPS measurements reveal the dynamic change in the surface composition of 10% Co–CZ catalyst under various feed conditions. The results show that the metallic Co species (Co^0), obtained from reducing the calcined sample and regarded as the key catalytic component for C–C cleavage in ethanol–water reactions, are re-oxidized to CoO (Co^{2+}) by water or a mixture of water and ethanol.

Moreover, a separate XPS measurement was carried out to further characterize the re-oxidation/re-reduction behavior of the surface CoO_x species on the 10% Co–CZ catalyst. In Fig. 4c(a), the Co^{2+} and Co^{3+} features in the Co2p region indicate that the supported Co species in the 10% Co–CZ catalyst mostly remained in the oxide form following the pre-reduction step in H_2 at 350 °C. However, these surface CoO_x species were found to be very reactive with ethanol and almost completely reduced to metallic cobalt in ethanol at 450 °C, as can be seen in Fig. 4c (b). The H_2 produced from the decomposition or dehydrogenation of ethanol over the catalyst surfaces could be responsible for such a reduction of CoO_x in ethanol, although the detailed surface chemistry requires further study. When the feed conditions were changed to the higher water-to-ethanol ratio during the in situ measurement, the peak re-emerged within 780.0–781.0 eV, as shown in Fig. 4c (c), which indicates the formation of CoO (Co^{2+}). The slower development of the oxide peak in Fig. 4c (c) compared to that in Fig. 4a (d) is due to its shorter duration (i.e. shorter exposure time in the feed stream of water–ethanol mixture) and the lower H_2O concentration.

3.3. Catalytic C–C cleavage of ethanol over Co/CeO_2–ZrO_2 with surface re-oxidation/re-reduction

Combining the results from our in situ studies using TPR and XPS, the formation of water-induced Co oxides is verified for pre-reduced 10% Co–CZ catalyst in steam or ethanol-steam conditions. Depending on the reaction temperature, the ceria species of 10% Co–CZ were observed to be simultaneously and perhaps cooperatively re-oxidized or re-reduced with the cobalt species. The re-oxidation/re-reduction between metallic Co and oxidized Co surface species was influenced by the feed composition (i.e. water-to-ethanol ratio).

The catalytic C–C cleavage of ethanol over the redox surfaces of the 10% Co–CZ catalyst was evaluated using different feed conditions in a packed-bed reactor. The catalyst was pre-reduced in situ under a hydrogen flow of 20 sccm at 450 °C for 2 h prior to testing. In the case of water-titrated catalyst, 0.033 ml of water was titrated at a flow rate of 0.2 ml/h before testing. After the pre-reduction or the pre-reduction/water titration, a mixture of ethanol and water with a water-to-ethanol ratio of 0 (ethanol only), 1, or 4 was fed in with a helium carrier gas at 450 °C, and the formation rate of gaseous products was measured time-on-stream. Fig. 5 shows the C1 production rates and the C–C cleavage conversions under ethanol decomposition (water-to-ethanol ratio of 0), water-assisted ethanol decomposition (water-to-ethanol ratio of 1), and ethanol steam reforming (water-to-ethanol ratio of 4) conditions. The data on the *x*-axis and *y*-axis were generated using the same operating conditions except that the pre-reduced catalyst was water-titrated for the *y*-axis data. All of the data points shown in Fig. 5 are aligned along the 45° line, indicating that the conversion of ethanol to C1 compounds was not significantly influenced

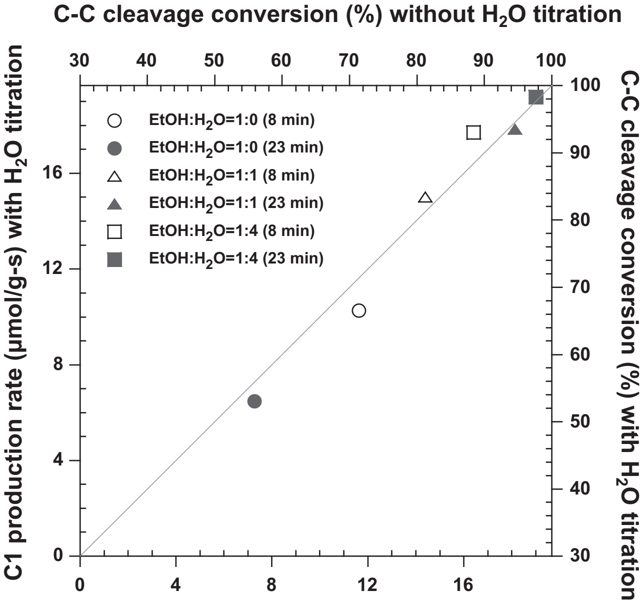

Fig. 5. Effect of the water titration process on C–C cleavage conversion and the C1 production rate over 10% $Co/CeO_2–ZrO_2$ catalysts in various ethanol–water mixtures. Ethanol was fed in at a constant weight hourly space velocity (WHSV) of 1.58 h^{-1} in all the streams. The catalysts were pre-reduced in H_2 at 450 °C for 2 h. In the case of the water-titrated catalyst, 0.033 ml of water was titrated at a flow rate of 0.2 ml/h before the catalyst testing.

by water titration, which gives the formation of the surface cobalt oxides.

As observed in Fig. 5, the initial state of the cobalt species, whether it has been exposed to water pre-treatment or not, has little effect on the C–C bond cleavage under ethanol-steam conditions. This result implies that the surface composition of the cobalt species in 10% Co–CZ catalyst, initially governed by the catalyst pre-treatments (e.g. H_2 pre-reduction or water titration), is transient and changes as the reaction proceeds, toward an equilibrium state governed by the composition of the reaction stream. This idea is supported by our findings from in situ XPS and TPR studies, in which the surface cobalt species changed reversibly from Co^0 to Co^{2+} when the water-to-ethanol ratio changed in the feed stream. For the supported cobalt with a composition of mixed metallic and oxidized Co resulting from partially reduced catalyst surfaces, the cobalt species became mostly Co^0 in an ethanol feed. For the catalyst pre-treated to have Co^0-rich surfaces, the exchange between the surface Co^0 and Co^{2+} species reached an equilibrium state depending on the water-to-ethanol ratio in the reaction stream. The various oxidation states of Co should give different catalytic abilities to break the C–C bond of ethanol. Thus, the 10% Co–CZ catalysts that contained different compositions of Co species initially showed different activities. However, as the surface composition reached equilibrium under the same reaction conditions, similar catalytic activities were obtained regardless of how the samples were pre-treated, as shown in Fig. 5.

4. Conclusions

The formation of water-induced cobalt oxides over 10% $Co/CeO_2–ZrO_2$ catalyst was verified by in situ measurements under various ethanol-steam conditions using TPR and XPS techniques. The surface analysis by XPS showed that these cobalt oxides were formed by re-oxidation of the metallic cobalt in the pre-reduced catalyst, wherein the redox exchange between reduced cobalt and oxidized cobalt occurred as the water-to-ethanol ratio changed in the feed stream. Also, the bulk reduction behaviors shown in our TPR study suggest two transient types for the water-induced cobalt oxides. The different reducibilities shown in these water-induced cobalt oxides are found to be associated with the catalysts' pre-reduction temperatures and the concentration of water in the reaction conditions (e.g. the feed composition). Furthermore, our TPR study indicates that the pre-reduction temperature determines the extent of interactions between supported cobalt species and $CeO_2–ZrO_2$ support, which could be the key step for determining what type of water-induced cobalt oxide is formed. The difficulty remains in identifying the true active centers for the cleavage of ethanol and the subsequent reactions, unless one can selectively and quantitatively control the formation of water-induced cobalt oxides in supported $Co/CeO_2–ZrO_2$ catalysts to measure the catalytic properties in the ethanol-steam conditions of interest.

Acknowledgments

This work was funded by the Berry Family Foundation and carried out in the O.H. Reaugh Laboratory for Oil and Gas Processing Research at Washington State University. A portion of the research was performed using EMSL, a national scientific user facility sponsored by the Department of Energy's Office of Biological and Environmental Research located at Pacific Northwest National Laboratory.

References

[1] S. Duan, S. Senkan, Industrial & Engineering Chemistry Research 44 (2005) 6381–6386.
[2] A. Haryanto, S. Fernando, N. Murali, S. Adhikari, Energy & Fuels 19 (2005) 2098–2106.
[3] M. Ni, D.Y.C. Leung, M.K.H. Leung, International Journal of Hydrogen Energy 32 (2007) 3238–3247.
[4] P.D. Vaidya, A.E. Rodrigues, Chemical Engineering Journal 117 (2006) 39–49.
[5] H. Idriss, Platinum Metals Review 48 (2004) 105–115.
[6] M. Mavrikakis, D.J. Doren, M.A. Barteau, Journal of Physical Chemistry B 102 (1998) 394–399.
[7] F. Haga, T. Nakajima, H. Miya, S. Mishima, Catalysis Letters 48 (1997) 223–227.
[8] J. Llorca, N. Homs, J. Sales, P.R. De la Piscina, Journal of Catalysis 209 (2002) 306–317.
[9] H. Song, L. Zhang, U.S. Ozkan, Green Chemistry 9 (2007) 686–694.
[10] D.R. Sahoo, S. Vajpai, S. Patel, K.K. Pant, Chemical Engineering Journal 125 (2007) 139–147.
[11] M.S. Batista, R.K.S. Santos, E.M. Assaf, J.M. Assaf, E.A. Ticianelli, Journal of Power Sources 134 (2004) 27–32.
[12] J.A. Anderson, M. Fernández Garcia, Supported Metals in Catalysis, vol. xii, World Scientific, NJ, 2005. 368 p.
[13] S.S.Y. Lin, D.H. Kim, S.Y. Ha, Catalysis Letters 122 (2008) 295–301.
[14] S.S.Y. Lin, D.H. Kim, S.Y. Ha, Applied Catalysis A – General 355 (2009) 69–77.
[15] J. Llorca, J.A. Dalmon, P.R. de la Piscina, N. Homs, Applied Catalysis A – General 243 (2003) 261–269.
[16] J. Llorca, P.R. de a Piscina, J.A. Dalmon, N. Homs, Chemistry of Materials 16 (2004) 3573–3578.
[17] V.A.D. O'Shea, N. Homs, E.B. Pereira, R. Nafria, P.R. de La Piscina, Catalysis Today 126 (2007) 148–152.
[18] S. Tuti, F. Pepe, Catalysis Letters 122 (2008) 196–203.
[19] A.K. Dalai, B.H. Davis, Applied Catalysis A – General 348 (2008) 1–15.
[20] D. Schanke, A.M. Hilmen, E. Bergene, K. Kinnari, E. Rytter, E. Adnanes, A. Holmen, Energy & Fuels 10 (1996) 867–872.
[21] A. Tavasoli, R.M.M. Abbaslou, A.K. Dalai, Applied Catalysis A – General 346 (2008) 58–64.
[22] J. van de Loosdrecht, B. Bazhinimaev, J.A. Dalmon, J.W. Niemantsverdriet, S.V. Tsybulya, A.M. Saib, P.J. van Berge, J.L. Visagie, Catalysis Today 123 (2007) 293–302.
[23] A.M. Saib, A. Borgna, J.V. De Loosdrecht, P.J. Van Berge, J.W. Niemantsverdriet, Journal of Physical Chemistry B 110 (2006) 8657–8664.
[24] S.S.Y. Lin, H. Daimon, S.Y. Ha, Applied Catalysis A – General 366 (2009) 252–261.
[25] G. Jacobs, R.A. Keogh, B.H. Davis, Journal of Catalysis 245 (2007) 326–337.
[26] H.H. Kung, Transition Metal Oxides: Surface Chemistry and Catalysis, vol. xi, Elsevier, Distributors for the US and Canada, Elsevier Science Pub. Co., Amsterdam, Netherlands, New York, NY, USA, 1989. 285 p.
[27] C. Li, Y. Sakata, T. Arai, K. Domen, K. Maruya, T. Onishi, Journal of the Chemical Society – Faraday Transactions I 85 (1989) 929–943.